Supplementary Information

Invasive FoxM1 phosphorylated by PLK1 induces the polarization of tumor-associated macrophages to promote immune escape and metastasis, amplified by IFITM1

Rong Xu[1], Young-Joo Lee[1], Chang-Hyeon Kim[1], Ga-Hong Min[1], Jung-Won Park[1], Yeo-Bin Kim[1], Dae-Hoon Kim[1], Jung-Hyun Kim[2], and Hyungshin Yim[1,*]

[1]Department of Pharmacy, College of Pharmacy, Institute of Pharmaceutical Science and Technology, Hanyang University, Ansan, Gyeonggi-do 15588, Republic of Korea

[2]Division of Intractable Diseases Research, Department of Chronic Diseases Convergence Research, Korea National Institute of Health, Cheongju, Chungcheongbuk-do 28160, Republic of Korea

[*]Corresponding author
Hyungshin YIM
Address: Department of Pharmacy, College of Pharmacy, Institute of Pharmaceutical Science and Technology, Hanyang University, Ansan, Gyeonggi-do 15588, Republic of Korea
Phone: +82-31-400-5810
FAX: +82-31-400-5958
E-mail: hsyim@hanyang.ac.kr

Supplementary Figure S1

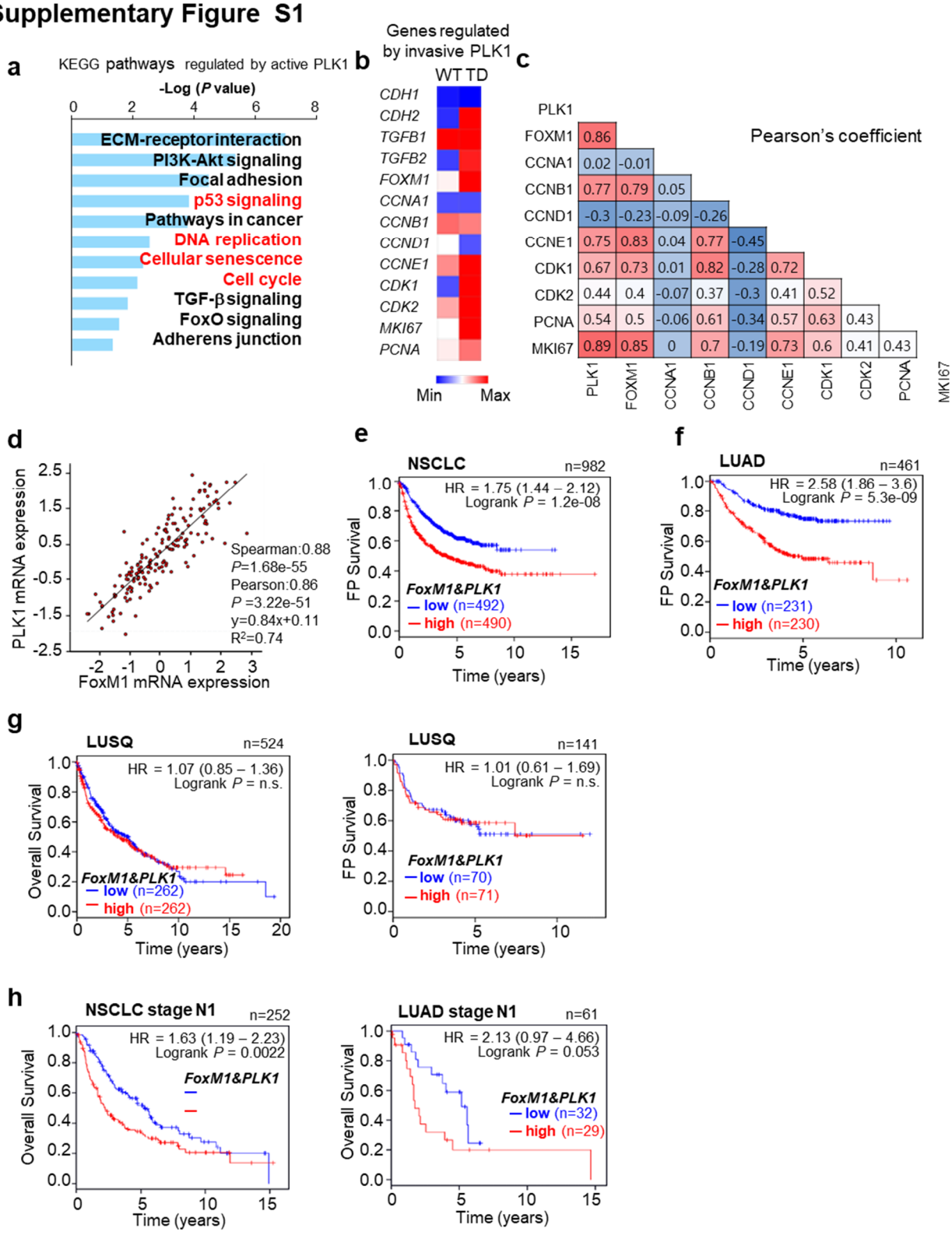

Supplementary Figure S1. Concurrent upregulation of FoxM1 and PLK1 is correlated

with poor survival of LUAD patients. a, Analysis of KEGG pathways regulated by active PLK1 extracted from the microarray data[1]. **b,** A heatmap analysis was performed from cell cycle-regulatory genes regulated by invasive PLK1 using the microarray data[1]. **c,** Analysis of Pearson's coefficient for the correlations between cell cycle-regulatory factors *PLK1*, *FOXM1*, *CCNA1*, *CCNB1*, *CCND1*, *CCNE1*, *CDK1*, *CDK2*, *PCNA*, and *MKI67* in non-small cell lung cancer (NSCLC) patients using cBioPortal. **d,** Analysis of Spearman's and Person's coefficients for correlations between *PLK1* and *FOXM1* in NSCLC patients using cBioPortal. **e-f,** Survival until first progression (FPS) rates of patients with NSCLC or LUAD were correlated with the levels of *FOXM1* and *PLK1* expression. FPS times of patients with NSCLC (n = 982) (**e**) and LUAD (n = 461) (**f**) were analyzed according to *PLK1* and *FOXM1* expression levels. High (Hi) *vs* low (Lo) expression was split by median cut-off value using KM plot database[2]. **g,** Overall survival rates (left) and FPS times (right) of patients with lung squamous cell carcinoma (LUSQ) were analyzed according to *PLK1* and *FOXM1* expression. High (Hi) *vs* low (Lo) expression was split by median cut-off value using KM plot database[2]. **h,** Overall survival rates of patients with TNM stage N1 NSCLC (left) and LUAD (right) were analyzed according to *PLK1* and *FOXM1* expression. High (Hi) *vs* low (Lo) expression was split by median cut-off value using KM plot database[2].

Supplementary Figure S2

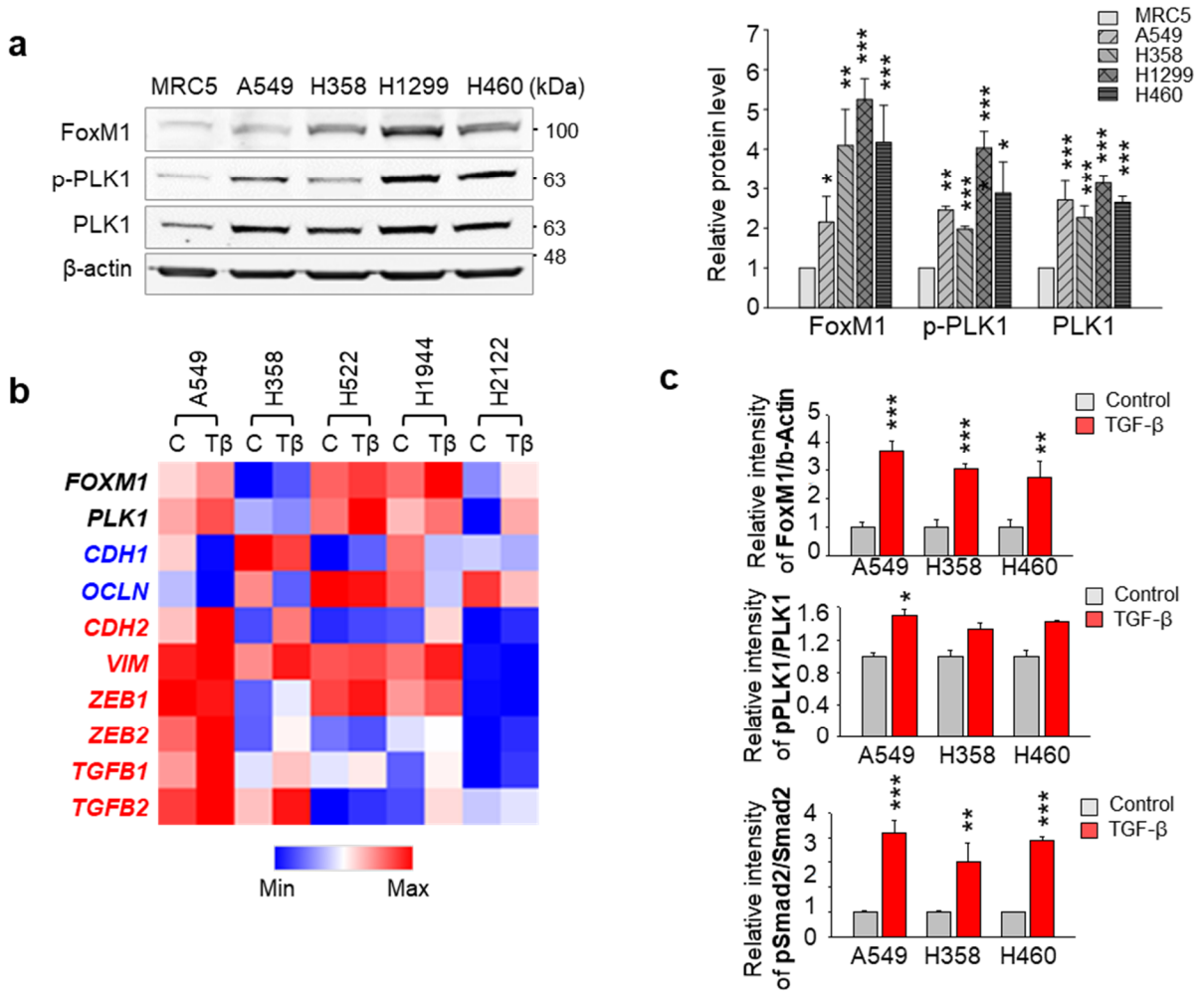

Supplementary Figure S2. Concurrent upregulation of FoxM1 and PLK1 in TGF-β-induced EMT. a, Immunoblotting was performed to measure the expression and phosphorylation of PLK1 using specific antibodies for FoxM1, PLK1, and p-PLK1 (T210) in A549, NCI-H358 (H358), NCI-H1299 (H1299), and NCI-H460 (H460) cells (left panel). The relative band intensities for FoxM1, p-T210-PLK1, and PLK1 were quantified using LI-COR Odyssey software (right panel). **b,** A heatmap analysis was performed from EMT-associated genes regulated by invasive PLK1. **c,** The relative band intensities of **Fig. 1f** for FoxM1/β-actin, p-T210-PLK1/PLK1, and p-Smad2 (S465/S467)/Smad2 were quantified using LI-COR Odyssey software.

Supplementary Figure S3

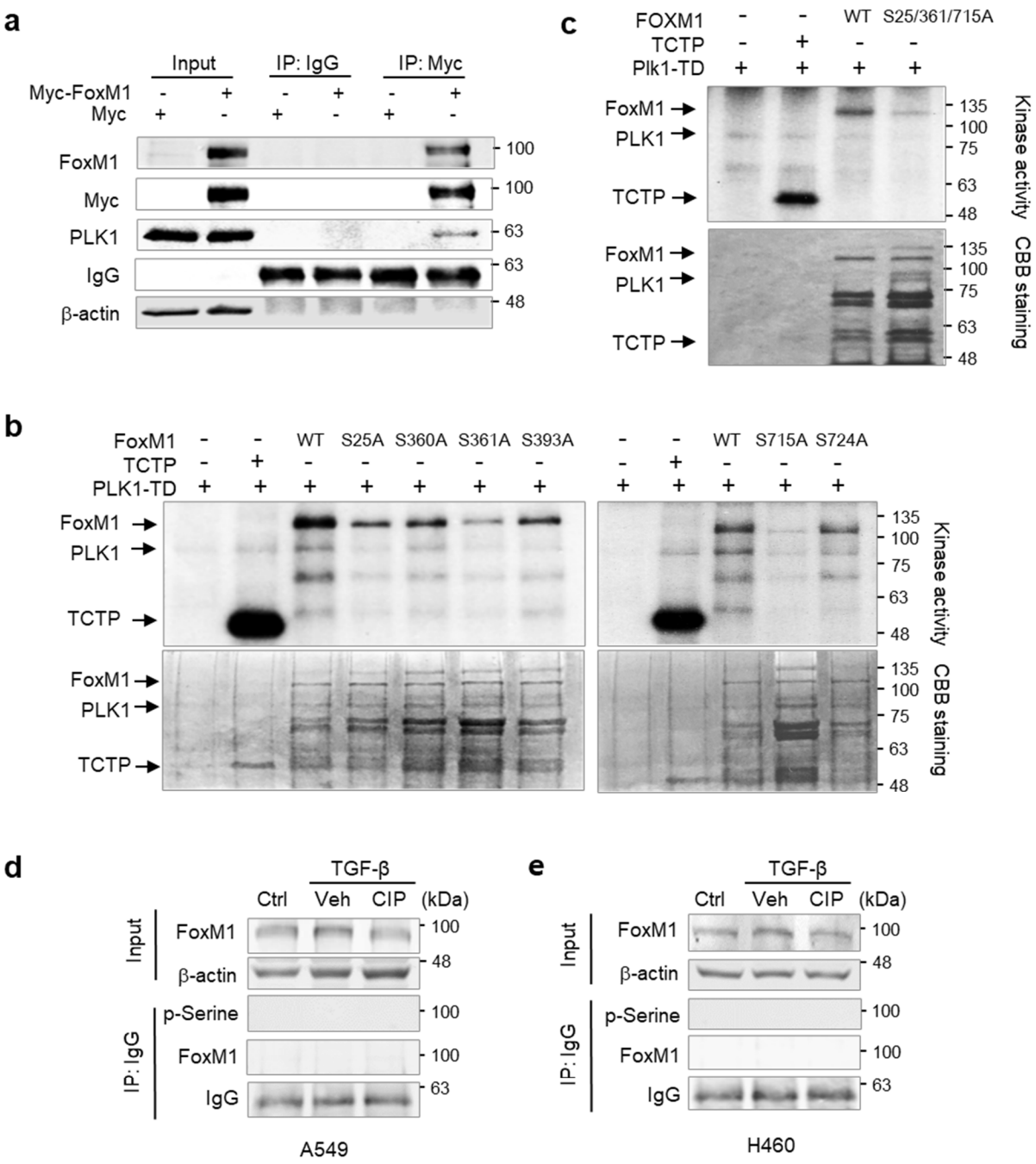

Supplementary Figure S3. TGF-β-induced EMT resulted in phosphorylation of FoxM1 by PLK1 by direct interaction. a, Myc-tagged FoxM1 was expressed in A549 cells. Immunoprecipitation of cell lysates was performed with normal IgG or anti-Myc antibodies and immunoblotting was done with anti-FoxM1, anti-Myc, and anti-PLK1 antibodies. **b,** An *in vitro* kinase assay was performed with active PLK1 (PLK1-TD), radioactive ATP, and purified GST-tagged FoxM1. GST-tagged FoxM1 was purified by site-directed single mutagenesis that substituted with alanine at S25, S360, S361, S393, S715, and S724 residues. GST-tagged TCTP was used as the positive control. **c,** An *in vitro* PLK1 kinase assay was performed with GST-tagged triple alanine mutant of FoxM1 at S25/S361/S715A (AAA) using radioactive ATP. **d-e**, Phosphorylation of FoxM1 occurred in A549 **(d)** and NCI-H460 **(e)** cells treated with TGF-β for 48 h. Treatment with calf intestinal alkaline phosphatase reduced the phosphorylation of FoxM1 in TGF-β-induced EMT. Immunoprecipitation of cell lysates was performed with anti-normal IgG or anti-FoxM1 (**Fig. 2f-g**) antibody and immunoblotting was done with anti-p-Serine antibodies. **f,** The possible residues on FoxM1 phosphorylated by PLK1 at the S25, S361, and S715 sites were evolutionarily conserved in several species including *Homo sapiens*, *Mus musculus*, *and Rattus norvegicus*.

Supplementary Figure S4

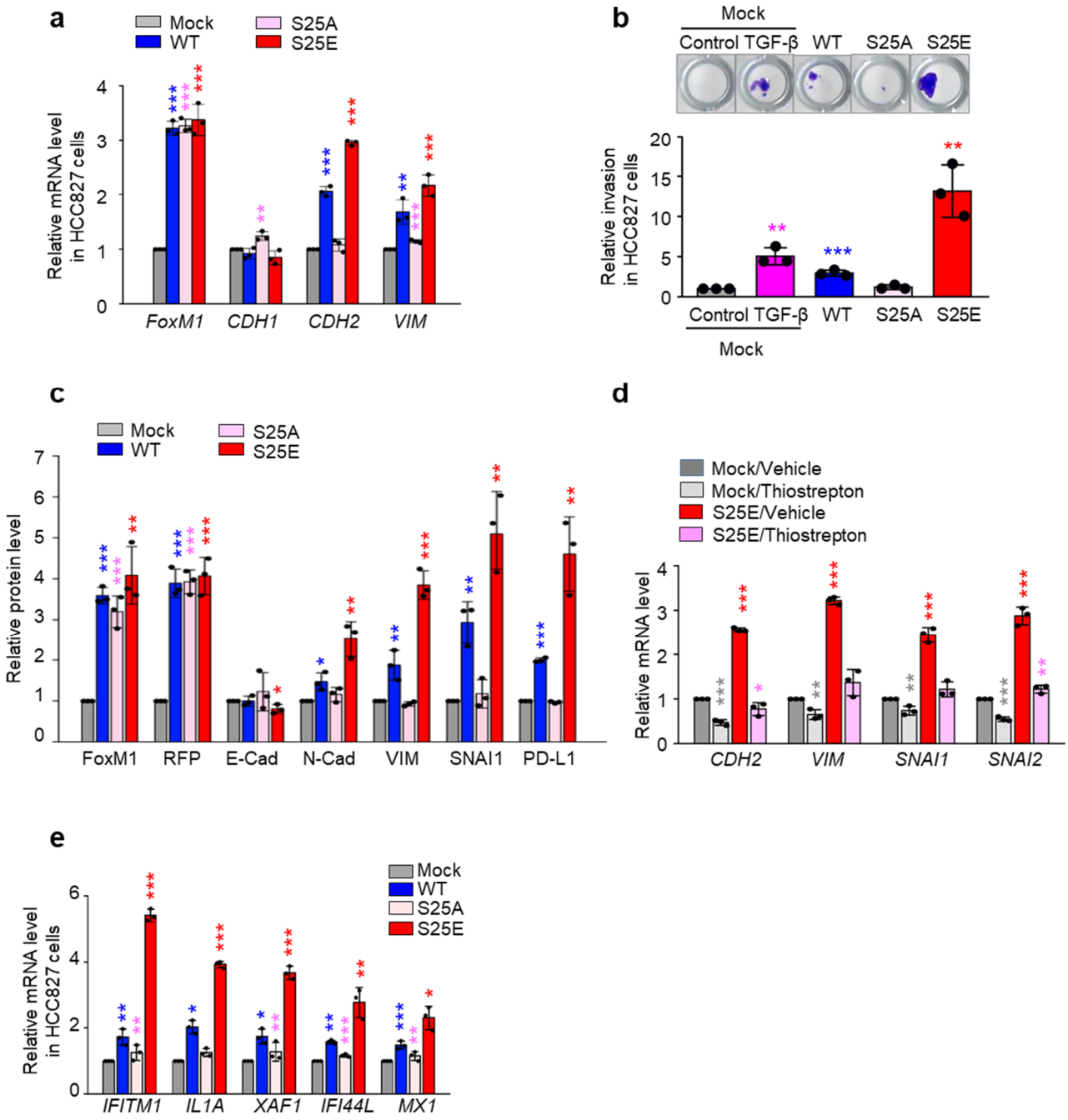

Supplementary Figure S4. Phosphorylation of FoxM1 at Ser25 facilitates the expression of mesenchymal genes, which are reduced by treatment with the FoxM1 inhibitor thiostrepton. a-b, RFP-tagged wild-type (WT) FoxM1 and S25A and S25E mutants were expressed in HCC827 cells. HCC827 cells were treated with doxycycline to express RFP-

tagged FoxM1. **a,** qRT-PCR was performed for *FOXM1*, *CDH1*, *CDH2*, and *VIM* in HCC827 cells expressing wild-type or mutants FoxM1. *$p < 0.05$; **$p < 0.01$; ***$p < 0.001$; ($n = 3$). Data are presented as mean ± SD. **b**, An invasion assay was performed using HCC827 cells expressing wild-type or mutants of FoxM1. Fourteen days after seeding, the cells that invaded the bottom surface were stained with 0.05% crystal violet dye, and the relative absorbance was plotted. Data are presented as mean ± SD of at least three independent experiments (significantly different from the experimental control). *$p < 0.05$; **$p < 0.01$; ***$p < 0.001$ compared with experimental control. **c,** A549 cells expressing RFP-tagged wild-type (WT), S25A, and S25E of FoxM1 were injected intravenously into the tail-veins of four-week-old BALB/c nude mice, and the tumorigenic and metastatic properties were evaluated after 15 weeks. Immunoblotting was performed using lung tissue lysates from each mouse model. The band intensity values of **Fig. 4d** were quantified using LI-COR Odyssey software, normalized, and plotted (right panel). **d**, A549 cells RFP-tagged WT, S25A, and S25E of FoxM1 were expressed in A549 cells. 5 μM Thiostrepton, a FoxM1 inhibitor, was applied for 48 h. qRT-PCR was performed for *CDH2*, *VIM*, *SNAI1*, and *SNAI2*. *$p < 0.05$; **$p < 0.01$; ***$p < 0.001$; ($n = 3$). Data are presented as mean ± SD. **e**, qRT-PCR was performed for the top five genes *IFITM1*, *XAF1*, *IF44L*, *MX1*, and *IL1A* in total HCC827 cells expressing FoxM1. *$p < 0.05$; **$p < 0.01$; ***$p < 0.001$; ($n = 3$). Data are presented as mean ± SD.

Supplementary Figure S5

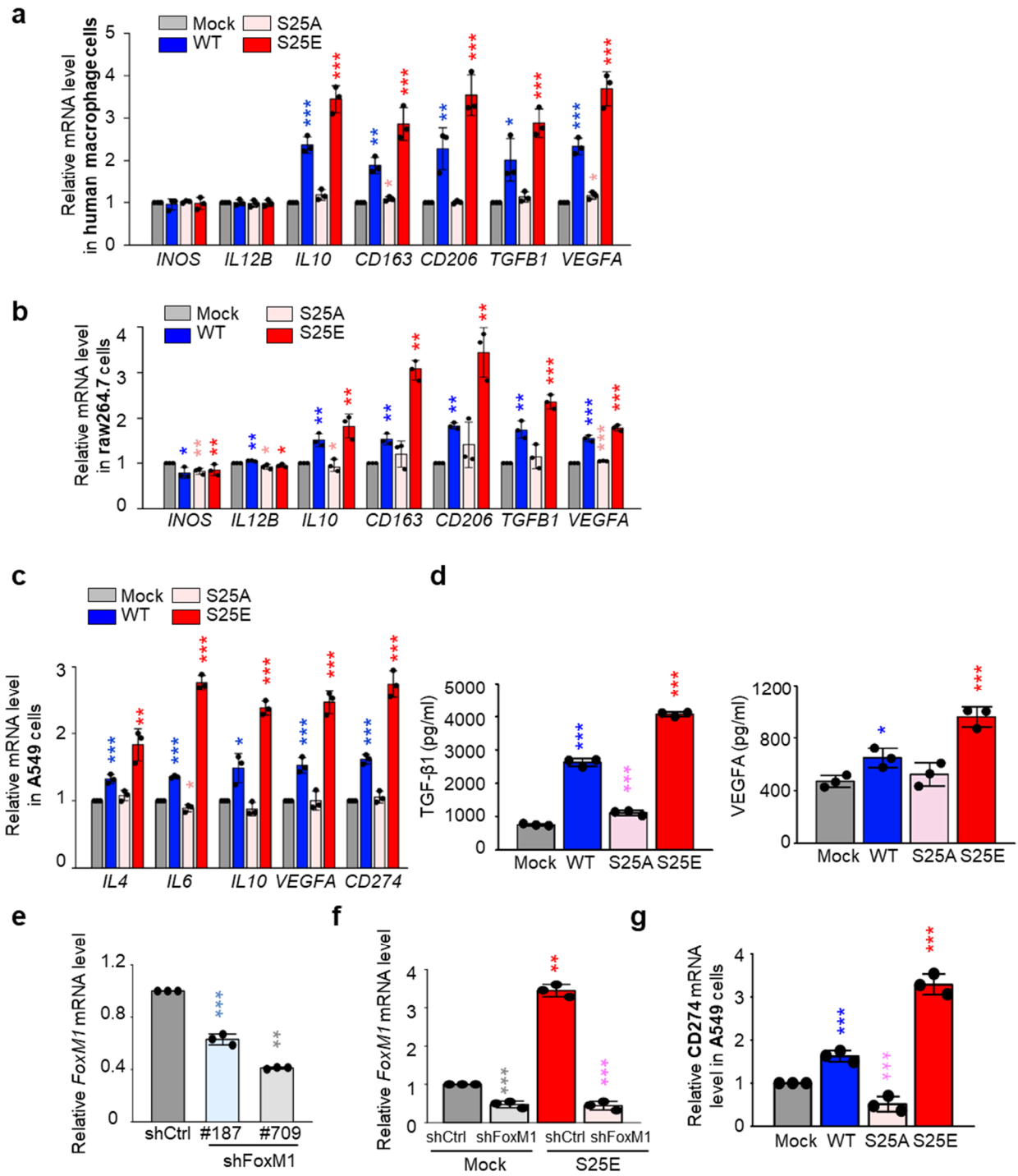

Supplementary Figure S5. p-FoxM1^{S25} functions in polarization of M2-like TAM and PD-L1 expression for cancer survival. a, Primary human macrophages derived from human pluripotent stem cells were co-cultured with A549 cells expressing mock, wild-type (WT), S25A, and S25E FoxM1 for 48 h. qRT-PCR was performed using co-cultured primary human macrophages for markers of M1 (*INOS*, *IL12B*), M2 (*IL10*, *CD163*, *CD206*), and TAM (*TGFB1*, *VEGFA*). **b**, Raw264.7 cells were co-cultured with A549 cells expressing mock, wild-type (WT), S25A, and S25E FoxM1 for 48 h. qRT-PCR was performed using co-cultured Raw264.7 cells for markers of M1 (*INOS*, *IL12B*), M2 (*IL10*, *CD163*, *CD206*), and TAM (*TGFB1*, *VEGFA*) **c**, Primary human macrophages were co-cultured with A549 cells expressing mock, WT, S25A, and S25E FoxM1. In A549 cells, qRT-PCR was performed for *IL4*, *IL6*, *IL10*, *VEGFA*, and *CD274*. **d**, HCC827^{S25E} cells were co-cultured with human THP macrophage cells. The secreted levels of TGF-β1 and VEGFA from human THP macrophages co-cultured with A549 cells were detected using ELISA. **e**, FoxM1 shRNA targeting at the position of 187–207 or 709–729 was applied to A549 cells. qRT-PCR was performed for *FOXM1*. $^{**}p < 0.01$; $^{***}p < 0.001$; ($n = 3$). **f**, A549 cells expressing mock, WT, S25A, and S25E FoxM1 were treated with FoxM1 shRNA (#709) for 48 h, and qRT-PCR was performed for *FOXM1*. $^{**}p < 0.01$; $^{***}p < 0.001$; ($n = 3$). **g**, A549 cells expressing mock, WT, S25A, and S25E FoxM1. qRT-PCR was performed for *CD274*. (Significantly different from the experimental control). $^{***}p < 0.001$; ($n = 3$). Data are presented as mean ± SD.

Supplemental Figure S6

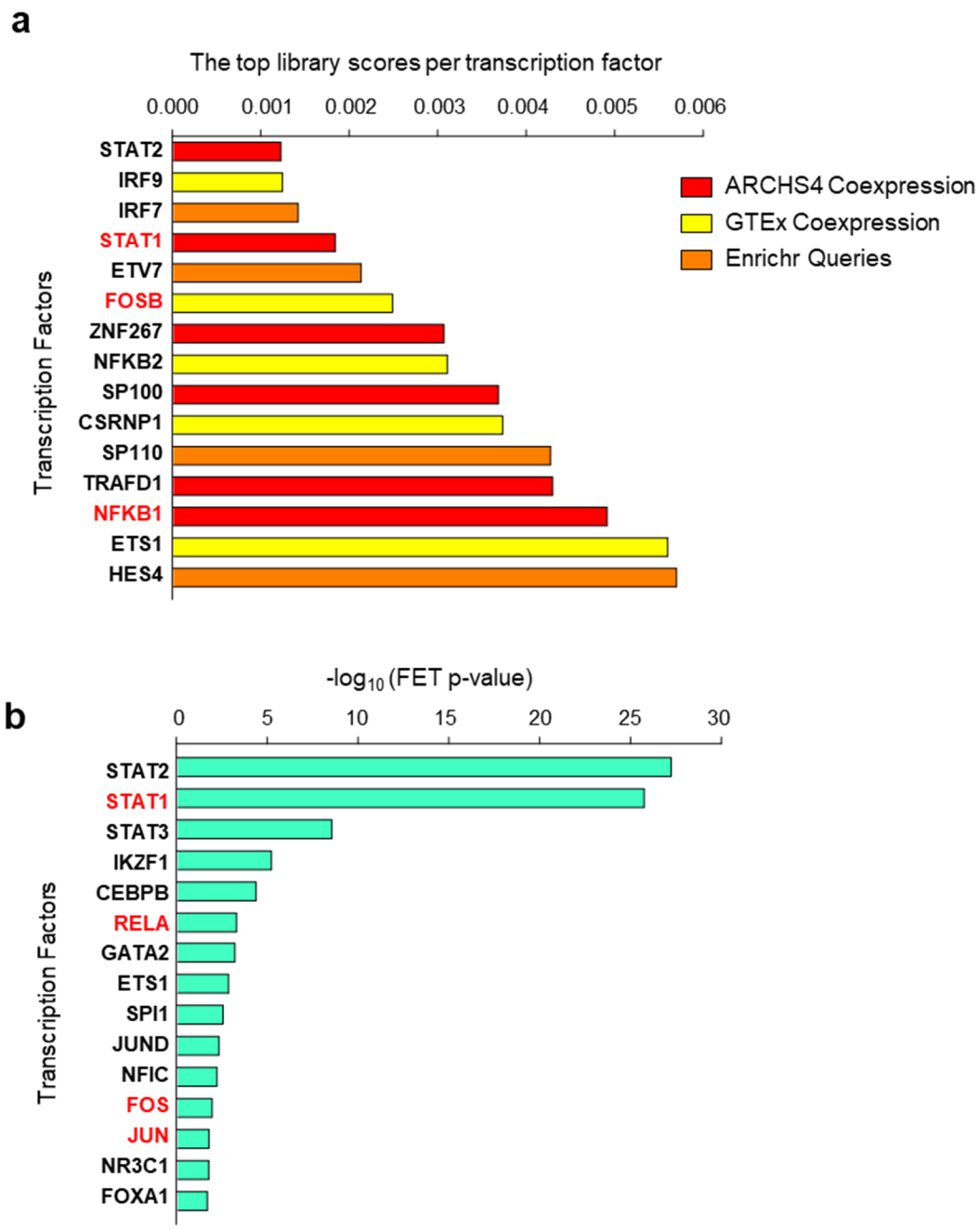

Supplementary Figure S6. Prediction of transcription factors in invasive cells having phosphorylated FoxM1 at S25. Using non-invasive and invasive A549 cells expressing S25E of FoxM1, transcriptome profiles were analyzed by microarray. The transcriptome data were clustered by gene probes with fold change >2 in cells expressing S25E FoxM1. The prediction

of transcription factors for these genes was performed by Appyter database[3]. Top ranked transcription factors were displayed within 15 with 2 of library threshold. **a,** Bar chart of top ranks across all libraries. The top ranked transcription factors according to their top integrated score across all the libraries. **b,** Bar chart of scores based on FET p-values. Transcription factors ranked by the ENCODE ChIP seq gene set library.

Supplementary Figure S7

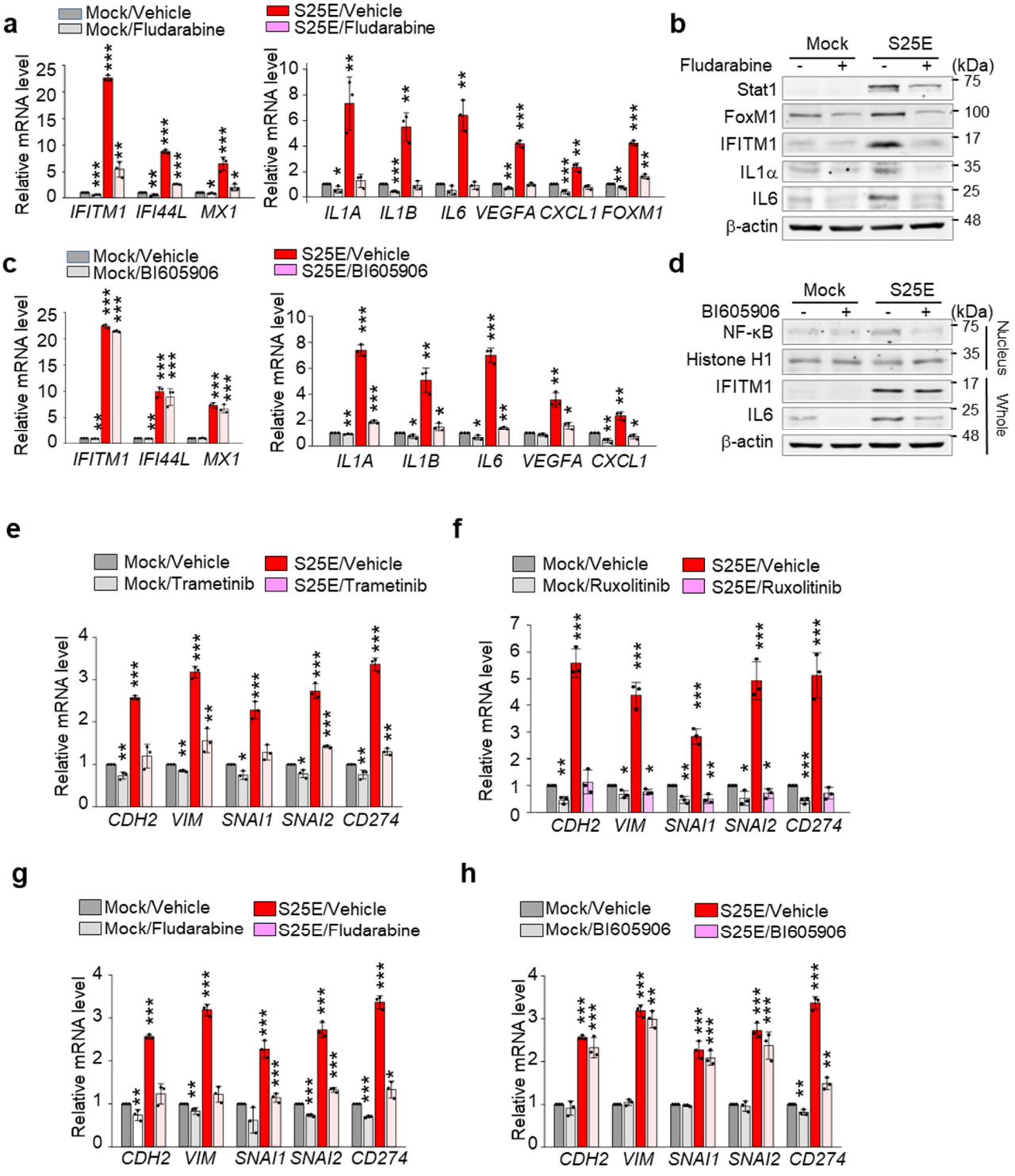

Supplementary Figure S7. p-FoxM1^{S25} upregulates the genes related to ISGs, TAM polarization, and EMT by MEK or JAK/STAT1 signaling. a-b, A549^{S25E} cells were treated with 1 μM fludarabin, a STAT1 inhibitor, for 48 h. **a**, qRT-PCR was performed for *IFITM1*, *IF44L*, *MX1*, *IL1A*, *IL1B*, *IL6*, *VEGFA*, *CXCL1*, and *FOXM1* in A549^{S25E} cells. **b**, Immunoblot analyses were performed using anti-FoxM1, anti-STAT1, anti-IFITM1, anti-IL1A, and anti-β-actin. **c-d,** A549^{S25E} cells were treated with 10 μM BI605906, an inhibitor of IKKβ, for 48 h. **c**, qRT-PCR was performed for *IFITM1*, *IF44L*, *MX1*, *IL1A*, *IL1B*, *IL6*, *VEGFA*, and *CXCL1* in A549^{S25E} cells. *$p < 0.05$; **$p < 0.01$; ***$p < 0.001$. Data are presented as mean ± SD. **d**, Immunoblotting was performed using whole and nuclear lysates of A549^{S25E} cells. Anti-NF-kB, anti-IFITM1, anti-IL1A, and anti-β-actin antibodies were used. Histone H1, a nuclear loading marker. **e-h,** A549 cells expressing S25E FoxM1 were treated with 1 μM trametinib (**e**), 15 μM ruxolitinib (**f**), 1 μM fludarabin (**g**), and 10 μM BI605906 (**h**) for 48 h. qRT-PCR was performed for *CDH2*, *VIM*, *SNAI1*, *SNAI2*, and *CD274*. *$p < 0.05$; **$p < 0.01$; ***$p < 0.001$. Data are presented as mean ± SD.

Supplementary Figure S8

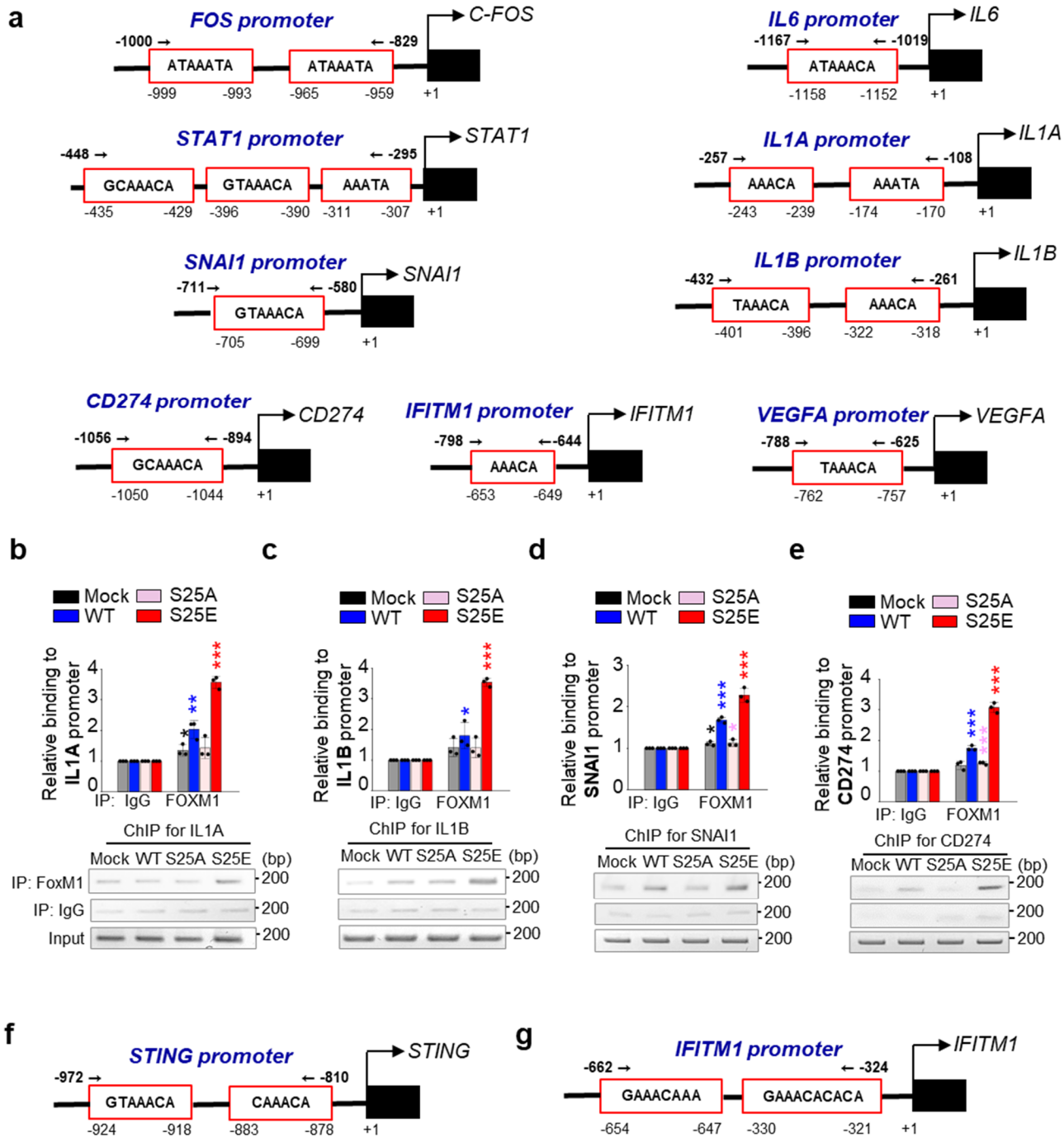

Supplementary Figure S8. p-FoxM1^{S25} upregulates the genes related to immune escape, TAM polarization, and EMT by direct activation. a, Scheme of promoter regions of *IFITM1*, *C-FOS*, *STAT1*, *CD274, IL6*, *IL1A*, *IL1B*, and *SNAI1*. FoxM1 binds to the region of A/G-C/T-

AAA-C/T-A sequences[4]. **b-e,** ChIP assays for FoxM1 binding to promoters of *IL1A* (**b**), *IL1B* (**c**), *SNAI1* (**d**), or *CD274* (**e**). Assays were performed on chromatin fragments using antibody to FoxM1 and normalized to pre-immune normal IgG. Immunoprecipitated fractions were assayed by PCR for binding to the promoters of *IL1A* (**b**), *IL1B* (**c**), *SNAI1* (**d**), or *CD274* (**e**). The PCR products were visualized in agarose gel. **f,** Scheme of promoter regions of *STING* for binding FoxM1 to the region of A/G-C/T-AAA-C/T-A sequences[4]. **g,** Scheme of *IFITM1* promoter regions for binding IRF3 to the region of 5'-GAAA(G/C)(G/C)GAAA-3' sequences[5] of interferon-sensitive response element (ISRE).

Supplementary Figure S9

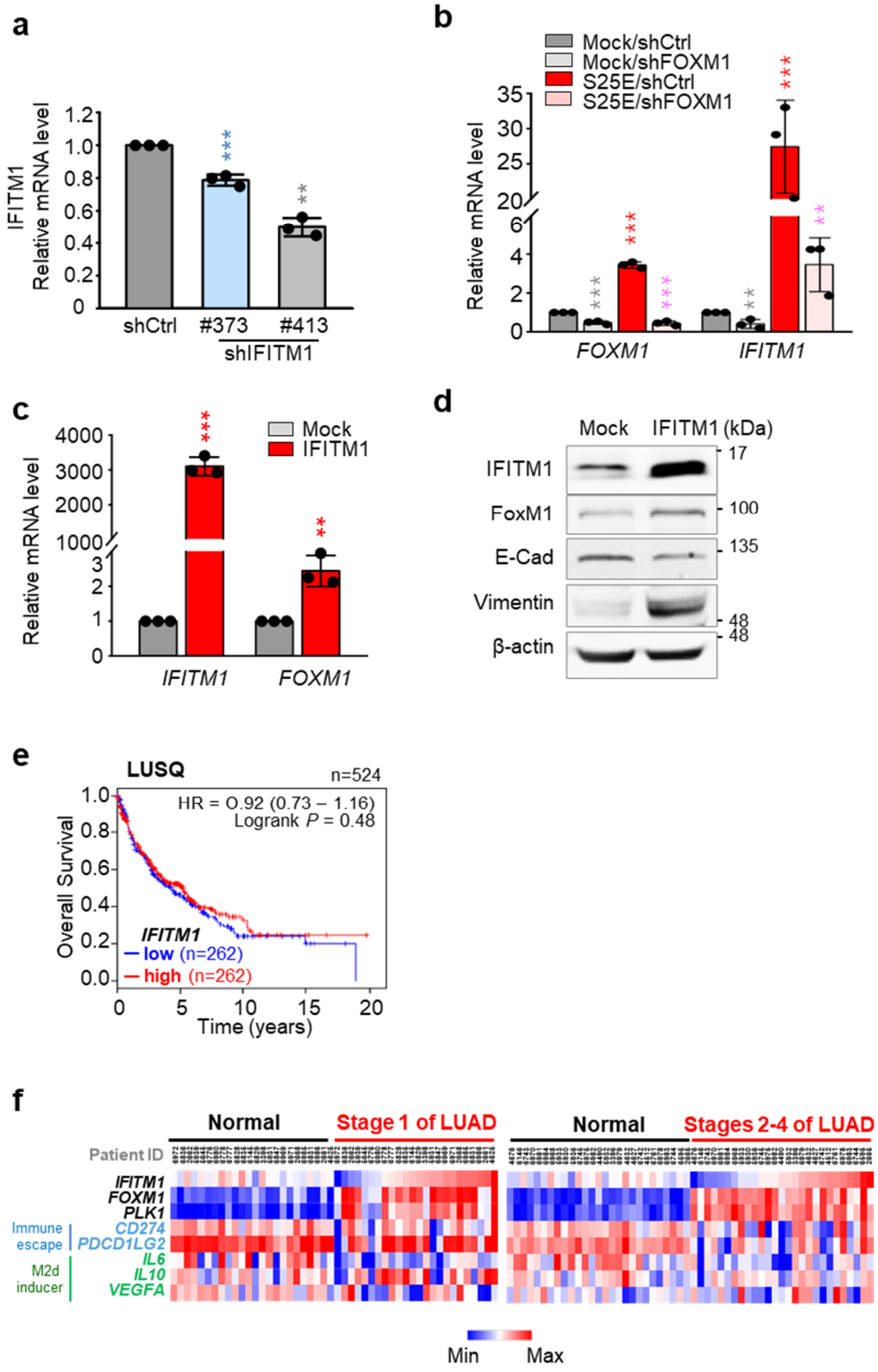

Supplementary Figure S9. IFITM1 functions as a regulator of metastasis and polarization of M2d-TAM in p-FoxM1-induced metastasis. a, IFITM1 shRNA targeting at the 373–393 or 413–433 position was treated with A549 cells. qRT-PCR was performed for *IFITM1*. $^{**}p < 0.01$; $^{***}p < 0.001$; ($n = 3$). **b,** FoxM1 shRNA was treated with A549 cells expressing S25E FoxM1 for 48 h. qRT-PCR was performed for *FOXM1* and *IFITM1*. $^{**}p < 0.01$; $^{***}p < 0.001$; ($n = 3$). **c-d,** IFITM1 plasmid was exogenously expressed in A549 cells for 40 h. The expression of FoxM1 and IFITM1 was observed using qRT-PCR (**c**) and immunoblot (**d**). **e,** Overall survival rates of patients in LUSQ were analyzed according to *IFITM1* expression level using KM PLOTTER. **f,** A heat map analysis showed the expression of genes *IFITM1*, *FOXM1*, *PLK1*, *CD274*, *PDCD1LG2*, *IL6*, *IL10*, and *VEGFA* based on the degree of expression of *IFITM1* from TCGA data analysis depending on stage of LUAD in normal and tumor tissue.

Supplementary Figure S10

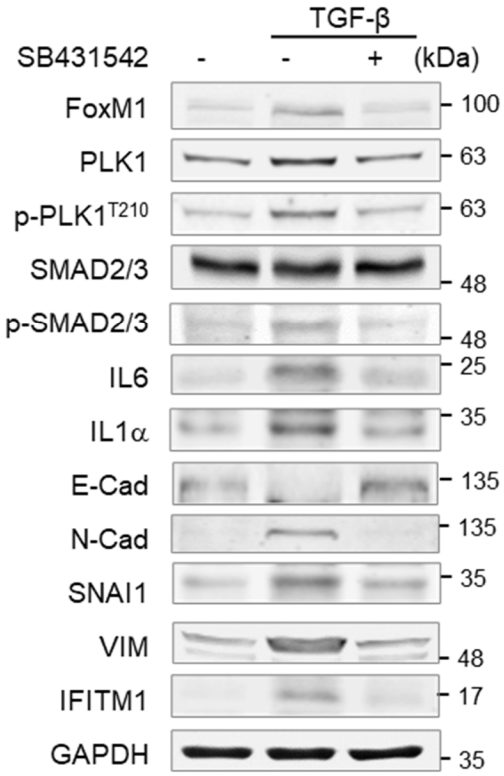

Supplementary Figure S10. TGF-β inhibitor SB431542 blocked the activation of PLK1 and levels of FoxM1, IL6, N-Cadherin, SNAI1, vimentin, and IFITM1 in A549 cells. Immunoblotting was performed using A549 cells treated with TGF- β and/or its inhibitor SB431542. FoxM1, PLK1, p-PLK1, Smad2/3, p-Smad2/3, IL6, IL β, N-cadherin, SNAI1, vimentin, IFITM1, and GAPDH were detected using specific antibodies.

Supplementary Figure S11

Fig. 3a-b

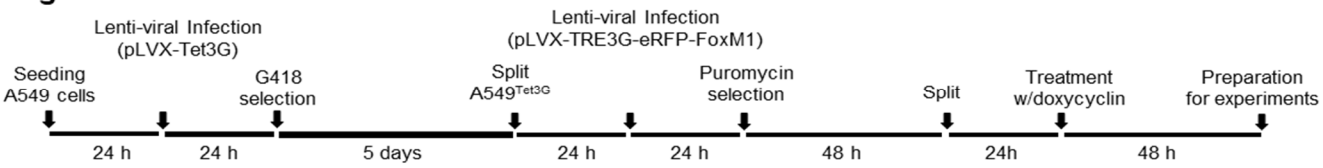

Fig. 3d

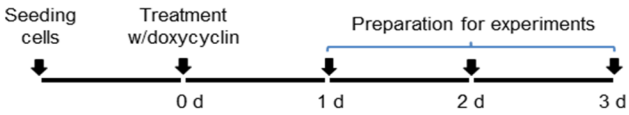

Fig. 3e

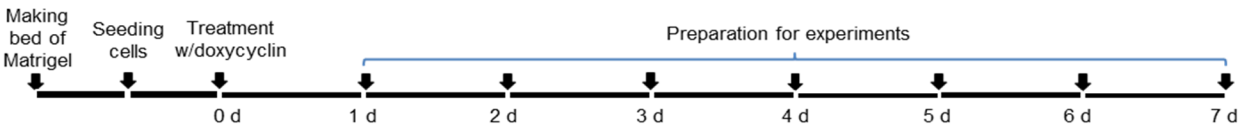

Fig. 4

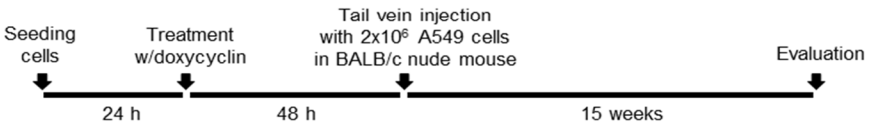

Fig. 6a-c, h-i

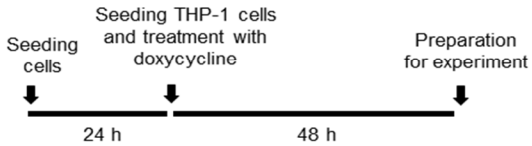

Fig. 6d

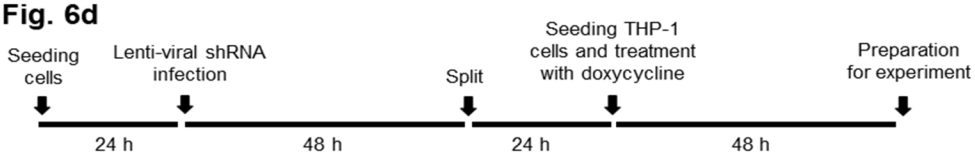

Fig. 8c-d

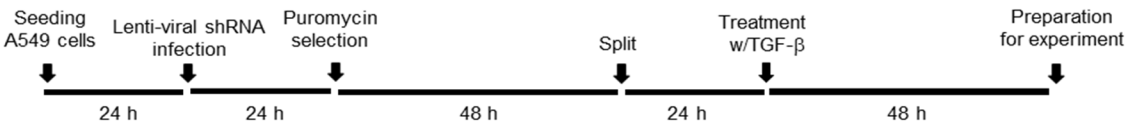

Supplementary Figure S11. Schemes of experiments.

Supplementary Tables

Supplementary Table S1. Analysis of Spearman's and Pearson's coefficients for the correlations between cell cycle-regulatory factors *PLK1*, *FOXM1*, *CCNA1*, *CCNB1*, *CCND1*, *CCNE1*, *CDK1*, *CDK2*, *PCNA*, and *MKI67* in non-small cell lung cancer (NSCLC) patients using cBioPortal used in Figure 1.

Genes	Spearman		Pearson	
	Coefficient	*P* value	Coefficient	*P* value
PLK1 & FOXM1	0.88	1.68E-55	0.86	3.22E-51
PLK1 & CCNA1	-0.01	0.896	0.02	0.749
PLK1 & CCNB1	0.81	7.40E-41	0.77	5.37E-35
PLK1 & CCND1	-0.24	1.54E-03	-0.3	8.77E-05
PLK1 & CCNE1	0.79	5.03E-37	0.75	7.67E-32
PLK1 & CDK1	0.68	1.09E-24	0.67	2.37E-23
PLK1 & CDK2	0.46	4.84E-10	0.44	1.44E-09
PLK1 & PCNA	0.53	2.07E-13	0.54	3.56E-14
PLK1 & MKI67	0.89	3.67E-59	0.89	1.13E-59
FOXM1 & CCNA1	-0.06	0.419	-0.01	0.858
FOXM1 & CCNB1	0.81	2.67E-41	0.79	6.43E-38
FOXM1 & CCND1	-0.15	0.0481	-0.23	2.84E-03
FOXM1 & CCNE1	0.84	3.51E-47	0.83	1.73E-44
FOXM1 & CDK1	0.71	2.25E-27	0.73	1.19E-29
FOXM1 & CDK2	0.43	4.71E-09	0.4	5.20E-08
FOXM1 & PCNA	0.48	2.41E-11	0.5	2.96E-12
FOXM1 & MKI67	0.87	1.87E-53	0.85	5.72E-48
CCNA1 & CCNB1	0.01	0.906	0.05	0.542
CCNA1 & CCND1	-0.1	0.191	-0.09	0.256
CCNA1 & CCNE1	0	0.985	0.04	0.643
CCNA1 & CDK1	-0.02	0.748	0.01	0.928
CCNA1 & CDK2	-0.11	0.165	-0.07	0.372
CCNA1 & PCNA	-0.07	0.346	-0.06	0.453

CCNA1 & MKI67	-0.05	0.522	0	0.958
CCNB1 & CCND1	-0.23	2.90E-03	-0.26	5.04E-04
CCNB1 & CCNE1	0.78	7.44E-36	0.77	2.09E-34
CCNB1 & CDK1	0.82	4.23E-42	0.82	7.23E-42
CCNB1 & CDK2	0.41	3.16E-08	0.37	6.08E-07
CCNB1 & PCNA	0.66	3.33E-22	0.61	2.15E-18
CCNB1 & MKI67	0.74	3.86E-31	0.7	1.05E-26
CCND1 & CCNE1	-0.33	1.45E-05	-0.45	1.07E-09
CCND1 & CDK1	-0.19	0.0117	-0.28	2.57E-04
CCND1 & CDK2	-0.14	0.0698	-0.3	6.80E-05
CCND1 & PCNA	-0.19	0.0143	-0.34	7.34E-06
CCND1 & MKI67	-0.15	0.0501	-0.19	0.0141
CCNE1 & CDK1	0.72	5.84E-28	0.72	2.58E-28
CCNE1 & CDK2	0.4	9.94E-08	0.41	3.56E-08
CCNE1 & PCNA	0.57	1.12E-15	0.57	3.97E-16
CCNE1 & MKI67	0.78	4.07E-35	0.73	3.11E-29
CDK1 & CDK2	0.5	3.54E-12	0.52	5.57E-13
CDK1 & PCNA	0.64	7.39E-21	0.63	3.06E-20
CDK1 & MKI67	0.63	8.86E-20	0.6	6.38E-18
CDK2 & PCNA	0.37	7.07E-07	0.43	3.84E-09
CDK2 & MKI67	0.43	5.09E-09	0.41	2.35E-08
PCNA & MKI67	0.44	2.44E-09	0.43	7.05E-09

1

2

Supplementary Table S2. Cox regression analysis for survival of non-small cell lung cancer (NSCLC) and lung adenocarcinoma (LUAD) patients expressing PLK1 and FOXM1 of KM plot used in Figure 1.

Patients	Endpoint	Gene expression	Number of patients (n)	Hazard ratio (HR)	95% Confidential interval (CI)
NSCLC	Overall Survival (OS) n=1885	$FOXM1^{Hi}/PLK1^{Hi}$	732	1.602	1.3822 ~ 1.857
		$FOXM1^{Hi}/PLK1^{Lo}$	212	1.673	1.3581 ~ 2.062
		$FOXM1^{Lo}/PLK1^{Hi}$	213	1.131	0.9022 ~ 1.417
		$FOXM1^{Lo}/PLK1^{Lo}$	728	-	-
LUAD	Overall Survival (OS) n=703	$FOXM1^{Hi}/PLK1^{Hi}$	260	2.172	1.6314 ~ 2.891
		$FOXM1^{Hi}/PLK1^{Lo}$	93	1.455	0.9862 ~ 2.147
		$FOXM1^{Lo}/PLK1^{Hi}$	93	1.030	0.6727 ~ 1.578
		$FOXM1^{Lo}/PLK1^{Lo}$	257	-	-
Stages 3-4 LUAD	Overall Survival (OS) n=137	$FOXM1^{Hi}/PLK1^{Hi}$	65	1.904	1.1501 ~ 2.550
		$FOXM1^{Hi}/PLK1^{Lo}$	13	0.804	0.3439 ~ 1.880
		$FOXM1^{Lo}/PLK1^{Hi}$	8	0.764	0.2289 ~ 2.550
		$FOXM1^{Lo}/PLK1^{Lo}$	51	-	-

Supplementary Table S3. Cox regression analysis for overall survival of lung adenocarcinoma (LUAD) patients expressing *PLK1*, *FOXM1*, and *IFITM1* of KM plot used in Figure 8I.

Tumor Stage	Gene expression	Number of patients (n)	Hazard ratio (HR)	95% Confidential interval (CI)
All (n=703)	$FOXM1^{Hi}/PLK1^{Hi}/IFITM^{Hi}$	156	2.236	1.5299 ~ 3.267
	$FOXM1^{Hi}/PLK1^{Hi}/IFITM^{Lo}$	104	2.337	1.5658 ~ 3.488
	$FOXM1^{Hi}/PLK1^{Lo}/IFITM^{Hi}$	49	1.599	0.9539 ~ 2.680
	$FOXM1^{Hi}/PLK1^{Lo}/IFITM^{Lo}$	44	1.440	0.8181 ~ 2.536
	$FOXM1^{Lo}/PLK1^{Hi}/IFITM^{Hi}$	40	1.224	0.6675 ~ 2.244
	$FOXM1^{Lo}/PLK1^{Hi}/IFITM^{Lo}$	53	0.980	0.5498 ~ 1.748
	$FOXM1^{Lo}/PLK1^{Lo}/IFITM1^{Hi}$	109	1.121	0.7075 ~ 1.776
	$FOXM1^{Lo}/PLK1^{Lo}/IFITM1^{Lo}$	148	-	-
Stages 3-4 (n=137)	$FOXM1^{Hi}/PLK1^{Hi}/IFITM^{Hi}$	32	2.439	1.2065 ~ 4.931
	$FOXM1^{Hi}/PLK1^{Hi}/IFITM^{Lo}$	33	1.751	0.8420 ~ 3.643
	$FOXM1^{Hi}/PLK1^{Lo}/IFITM^{Hi}$	6	1.597	0.5545 ~ 4.599
	$FOXM1^{Hi}/PLK1^{Lo}/IFITM^{Lo}$	7	0.400	0.0894 ~ 1.788
	$FOXM1^{Lo}/PLK1^{Hi}/IFITM^{Hi}$	4	3.335	0.7223 ~ 15.384
	$FOXM1^{Lo}/PLK1^{Hi}/IFITM^{Lo}$	4	0.318	0.0416 ~ 2.439
	$FOXM1^{Lo}/PLK1^{Lo}/IFITM^{Hi}$	28	1.174	0.5057 ~ 2.725
	$FOXM1^{Lo}/PLK1^{Lo}/IFITM^{Lo}$	23	-	-

Supplementary Table S4. Sequences of forward (F) and reverse (R) primers used for qRT-PCR amplification.

Target Gene	Primer	Sequences
Human *FOXM1*	Forward	5'-TGGACCAGGTGTTTAAGCAGC-3'
	Reverse	5'-CCGGGAGACGTCTGCCAATGG-3'
Human *PLK1*	Forward	5'- AAGAGATCCCGGAGGTCCTA -3'
	Reverse	5'- TCATTCAGGAAAAGGTTGCC -3'
Human *CDH1*	Forward	5'- ACCACCTCCACAGCCACC -3'
	Reverse	5'- GTCCAGTTGGCACTCGCC -3'
Human *CDH2*	Forward	5'- ACAGTGGCCACCTACAAAGG -3'
	Reverse	5'- CCGAGATGGGGTTGATAATG -3'
Human *VIM*	Forward	5'- GAGAACTTTGCCGTTGAAGC -3'
	Reverse	5'- GCTTCCTGTAGGTGGCAATC -3'
Human *SNAI1*	Forward	5'- GGAAGCCTAACTACAGCGAG -3'
	Reverse	5'- CAGAGTCCCAGATGAGCATTG -3'
Human *SNAI2*	Forward	5'- ACGCCCAGCTACCCAATG -3'
	Reverse	5'- AGGGCGCCCAGGCTCACATA -3'
Human *ZEB1*	Forward	5'-TGGGATCAACCACCAATGG-3'
	Reverse	5'-AAGTAACCCTGTGTATTTCTGGATGA-3'
Human *TWIST*	Forward	5'- GGACAAGCTGAGCAAGATTCAGA-3'
	Reverse	5'- TCTGGAGGACCTGGTAGAGGAA -3'
Human *IFITM1*	Forward	5'-TCAACACCCTCTTCTTGAAC-3'
	Reverse	5'-AGAGCCGAATACCAGTAACA-3'
Human *XAF1*	Forward	5'-TTCGTCCAAAGACAAGAAGT-3'
	Reverse	5'-CTCCTCAGAATGTCATAGGC-3'
Human *IL1A*	Forward	5'-AAGTCATCAAAGGATGATGC-3'
	Reverse	5'-AGAAGAAGAGGAGGTTGGTC-3'
Human *IL1B*	Forward	5'-GGGCCTCAAGGAAAAGAATC-3'
	Reverse	5'-TTCTGCTTGAGAGGTGCTGA-3'
Human *MX1*	Forward	5'-CAAAGGAACTGAAGACAAGG-3'
	Reverse	5'-GAAATATGGGTGGTTCTCAA-3'

Human *IFI44L*	Forward	5’-GTCTTGAAGAACCTCACTGC-3’
	Reverse	5’-GGATTCACTGTGTGGCTTAT-3’
Human *INOS*	Forward	5’-TATCACAACCTCAGCAAGCA-3’
	Reverse	5’-AAAATCCCTTTGGCCTTATG-3’
Human *IL12B*	Forward	5’-GGAGCTGCTACACTCTCTGC-3’
	Reverse	5’-GATGAAGAAGCTGCTGGTGT-3’
Human *IL4*	Forward	5’-ACATTGTCACTGCAAATCGACACC-3’
	Reverse	5’-TGTCTGTTACGGTCAACTCGGTGC-3’
Human *IL6*	Forward	5’-CAGACAGCCACTCACCTCTT-3’
	Reverse	5’-CTTTTTCAGCCATCTTTGGA-3’
Human *IL10*	Forward	5’-AACCAAGACCCAGACATCAA-3’
	Reverse	5’-TGGCTTTGTAGATGCCTTTC -3’
Human *CD163*	Forward	5’-TGATTCGGACTTCTCTCTGG-3’
	Reverse	5’-TGGCTACAAGTTCCTTCTGG-3’
Human *CD206*	Forward	5’-ACTGCAAGCTTCACAATTCC-3’
	Reverse	5’-ATTTCAATTTGGGCTCATCA-3’
Human *CD274*	Forward	5’-CAAAGAATTTTGGTTGTGGA-3’
	Reverse	5’-AGCTTCTCCTCTCTCTTGGA-3’
Human *TGFB1*	Forward	5’-GGGACTATCCACCTGCAAGA-3’
	Reverse	5’-CCTCCTTGGCGTAGTAGTCG-3’
Human *VEGFA*	Forward	5’-TTCCAGGAGTACCCTGATGA-3’
	Reverse	5’-TGAGGTTTGATCCGCATAAT-3’
Human *CD279*	Forward	5’-CGTGGCCTATCCACTCCTCA-3’
	Reverse	5’-ATCCCTTGTCCCAGCCACTC-3’
Human *CXCL1*	Forward	5’-ACCCCAAGAACATCCAAAGT -3
	Reverse	’5’-TGGATTTGTCACTGTTCAGC -3’
Human *GAPDH*	Forward	5’- TAAAGGGCATCCTGGGCTACACT -3’
	Reverse	5’- TTACTCCTTGGAGGCCATGTAGG -3’
Mouse *INOS*	Forward	5’-CCTGTGTTCCACCAGGAGAT-3’
	Reverse	5’-AGAGGACTGTGGCTCTGACC-3’
Mouse *IL12B*	Forward	5’-CTGCAGAGAAGGTCACACTG-3’
	Reverse	5’-TGATGATGTCCCTGATGAAG-3’

Mouse *IL10*	Forward	5’-CAGCCGGGAAGACAATAACT-3’
	Reverse	5’-TCATTTCCGATAAGGCTTGG-3’
Mouse *CD163*	Forward	5’-AGATTGCCTCATGACTGCTC-3’
	Reverse	5’-CACTTGCTATGCAGGGAACT-3’
Mouse *CD206*	Forward	5’-GAGCCTGTGAGCAACCACTA-3’
	Reverse	5’-TTTCATTTGTGCATGTGTGG-3’
Mouse *VEGFA*	Forward	5’-TTAAATCCTGGAGCGTTC-3’
	Reverse	5’-CACATCTGCAAGTACGTTCG-3’
Mouse *GAPDH*	Forward	5’-GTTGTCTCCTGCGACTTCA-3’
	Reverse	5’-GGTGGTCCAGGGTTTCTTA-3’

Supplementary Table S5. Sequences of forward (F) and reverse (R) primers used for site-directed mutagenesis for FoxM1.

Target Residue	Primer	Sequences
S25A	Forward	5'-CCTCCTCTGATGTTTCAGCTGGGGCATTTTGAACAGGAAG -3'
	Reverse	5'-CTTCTTGTTCAAAATGCCCCAGCTGAAACATCAGAGGAGG -3'
S25E	Forward	5'-CTTCCTGTTCAAAATGCCCCAGAGGAAACATCAGAGGAGGAACCT -3'
	Reverse	5'-AGGTTCCTCCTCTGATGTTTCCTCTGGGGCATTTTGAACAGGAAG -3'
S361A	Forward	5'-TAGGTACCAGGTATGCGCTGACCCGTGGTAG -3'
	Reverse	5'-CTACCACGGGTCAGCGCATACCTGGTACCTA -3'
S361E	Forward	5'-CTGCTACCACGGGTCAGCGAGTACCTGGTACCTATCCAG-3'
	Reverse	5'-CTGGATAGGTACCAGGTACTCGCTGACCCGTGGTAGCAG -3'
S715A	Forward	5'-AGCAGGATCTTGCTGAGGGCGTCATTCATTGTGTCCAG -3'
	Reverse	5'-CTGGACACAATGAATGACGCCCTCAGCAAGATCCTGCT -3'
S715E	Forward	5'-CCTGGACACAATGAATGACGAGCTCAGCAAGATCCTGCTGG -3'
	Reverse	5'-CCAGCAGGATCTTGCTGAGCTCGTCATTCATTGTGTCCAGG -3'

Supplementary Table S6. Sequences of forward (F) and reverse (R) primers used for ChIP assay.

Target Gene	Primer	Sequences
Human *IL6*	Forward	5'-TATAGGTGAATAAACAAG -3'
	Reverse	5'-CCTTTTCCCAGAGGTAGCAC -3'
Human *VEGFA*	Forward	5'-CGGGTTTTATCCCTCTTCTT -3'
	Reverse	5'-TTCTGCTGGTTTCCAAAATC -3'
Human *STAT1*	Forward	5'-AGTTTGGGCTTCTGCAAACA -3'
	Reverse	5'-CACGCGCTGGGGTATTTC -3'
Human *FOS*	Forward	5'-AATAAATGCGCTGTCTTCTTT -3'
	Reverse	5'-CAGACCTTCATCCCCTAACC -3'
Human *IL1A*	Forward	5'-CTGGAATATCTGCAAACAAC -3'
	Reverse	5'-TGGCTACGTGGCTACAAGTG -3'
Human *IL1B*	Forward	5'-CTGGAATATCTGCAAACAAC -3'
	Reverse	5'-TGGCTACGTGGCTACAAGTG -3'
Human *IFITM1*	Forward	5'-GGTTTTATTGAGCAGAGTGA -3'
	Reverse	5'-GCCTTTGTTTCTCTCTCTGG -3'
Human *SNAI1*	Forward	5'-CGCTCCGTAAACACTGGATA -3'
	Reverse	5'-AGGGAAACGCACATCACTG -3'
Human *CD274*	Forward	5'-GGAAAGGCAAACAACGAAGA -3'
	Reverse	5'-AGGGAAACGCACATCACTG -3'

Reference

1. Shin, S.B., Jang, H.R., Xu, R., Won, J.Y. & Yim, H. Active PLK1-driven metastasis is amplified by TGF-beta signaling that forms a positive feedback loop in non-small cell lung cancer. *Oncogene* **39**, 767-785 (2020).
2. Gyorffy, B., Surowiak, P., Budczies, J. & Lanczky, A. Online survival analysis software to assess the prognostic value of biomarkers using transcriptomic data in non-small-cell lung cancer. *PLoS One* **8**, e82241 (2013).
3. Clarke, D.J.B. *et al.* Appyters: Turning Jupyter Notebooks into data-driven web apps. *Patterns (N Y)* **2**, 100213 (2021).
4. Chen, X. *et al.* Targeting the CtBP1-FOXM1 transcriptional complex with small molecules to overcome MDR1-mediated chemoresistance in osteosarcoma cancer stem cells. *J Cancer* **12**, 482-497 (2021).
5. Andrilenas, K.K. *et al.* DNA-binding landscape of IRF3, IRF5 and IRF7 dimers: implications for dimer-specific gene regulation. *Nucleic Acids Res* **46**, 2509-2520 (2018).